

The present chapter deals with the experimental details about to the techniques employed for the chemical and structural characterizations of the additives, specification of steel ball bearing and testing methodologies used in the evaluation of lubrication performance of antiwear additives. The techniques used for studying the morphology of worn surfaces and tribochemistry of additives have also been discussed.

2.1. Instrumentation details:

2.1.1. Electronic Absorption Spectroscopy (UV-Visible)

UV-visible spectra of the additives were recorded in DMSO solution in the range 200-1100 nm on a Shimadzu Pharmaspec. UV-1700 model and LAMDA 25 Spectrophotometer Perkin Elmer, Germany.

2.1.2. Fourier Transform Infrared Spectroscopy (FTIR)

FTIR spectroscopy is one of the most important analytical techniques available to researchers. The FTIR spectra of all samples were recorded using SHIMADZU FTIR-8400S and PerkinElmer 100 spectrum spectrophotometer in the range 4000-400 cm^{-1} . The powder of each sample was mixed with KBr to form the pellets in order to scan FTIR spectra.

2.1.3. Nuclear Magnetic Resonance Spectroscopy (NMR)

NMR spectroscopy is used to confirm the identity of substance and gives distinguishable signals for identical functional groups with different neighbouring substituents. The chemical structure was confirmed by ^1H NMR spectra. NMR spectra of additives were recorded on JEOL AL 500 FT NMR operating at 500 and 75 MHz

resonance frequencies for ^1H NMR, respectively using CDCl_3 and DMSO-d_6 as solvents. All chemical shifts are reported in parts per million (ppm) down field from the internal reference Me_4Si , TMS.

2.1.4. Powder X-Ray Diffraction (XRD)

XRD is a rapid quantitative and qualitative technique primarily used to provide information about the phase identification, purity and size of crystalline material. The powder XRD patterns of all nanomaterials were examined using Bruker D8 Advance and XPERT-PRO diffractometer system with $\text{Cu K}\alpha$ radiation ($\lambda = 0.15418$ nm). The diffraction data were recorded for 2θ angles between 20° and 80° (step size 0.02, step time 1s) and collected spectra peaks were matched with peaks mentioned in JCPDS files. The d-spacing is calculated from the values of the peaks observed from Bragg's equation.

$$n\lambda = 2d \sin \theta \quad 2.1$$

Where, n is the order of reflection, and the values are 1, 2, 3,... λ is the wavelength of the X-ray radiation, d is the interlayer spacing between two successive planes and θ is the angle between the incident ray and the scattering planes. Knowing θ , n and λ , the lattice spacing d can be easily calculated.

2.1.5. Transmission Electron Microscopy (TEM)

TEM is a powerful characteristic tool to observe the morphological features such as shape, size, and crystallographic details of the material at high resolution. To analyse the structural features, dispersion of powdered sample in ethanol was mounted over the carbon-coated TEM grid and examined under a Technai-G² (FEI,

Eindhoven, Netherlands) electron microscope equipped with SIS Mega View III CCD camera (FEI, Eindhoven, Netherlands) at 120 kV. Measurements were done using AnalySIS software (SIS, Muenster, Germany).

2.1.6. X-ray Photoelectron Spectroscopy (XPS)

XPS is a quantitative and surface-sensitive spectroscopic technique that used to measure the elemental composition of the material and also gives information about the oxidation states of the associated elements. The X-ray Photoelectron Spectroscopy was used for analyzing the chemical composition of materials. Three different XPS spectrometers were used to record the samples. The radiation source Al K α line with the energy of (1486.6 eV) and the binding energy of C1s (284.6 eV) was used for the calibration of the spectrometer, VSW Scientific Instruments photoelectron spectrometer; Sigma Probe and Thermo VG Scientific spectrometer. The radiation source Mg K α line with a pass energy of 29.35 eV was used in case of AMICUS Kratos Analytical, Shimadzu, U.K.

2.1.7. Raman Spectroscopy

Raman spectroscopic measurements were carried out to confirm chemical and structural features of carbon- based nanomaterials. Raman spectra were obtained with a micro-Raman setup (HR LabRam inverse system, JobinYvon Horiba), the 532 nm line from a frequency-doubled Nd:YAG laser (Coherent Compass) was used as excitation wavelength.

2.1.8. Field Emission Scanning Electron Microscopy (FE-SEM)

In order to understand the morphological features of the synthesized additive, FE-SEM is a very prominent technique. Field Emission Scanning electron microscope (FE-SEM) images were recorded by field Emission scanning electron microscopy (FE-SEM) (FEI- Nova Nano SEM 450).

2.2. Computational Methodology

All models were constructed using the Materials and Processes Simulations Platform (MAPS version 4.0.1) from Scienomics SARL (Paris, France). The molecules required for making the four model systems were constructed using the MAPS molecule builder. Each molecule (OH-BT, OH-BTS, OH-NT, H-NT) in paraffin oil was first constructed by the MAPS molecular builder and then geometrically optimized by MNDO [42]. All molecules making the paraffin oil (PO), were modeled as a linear chain of alkanes consist of 56 atoms [$C_{18}H_{38}$]. The BCC Fe unit cell was used to construct the supercell, and then this was cleaved to obtain its (110) surface. The Fe (110) surface slab dimensions thus obtained were approximately $42.90\text{\AA} \times 42.90\text{\AA} \times 8.58\text{\AA}$. Fe (110) surface slab was placed normal to the z-axis of the simulation cell. It makes up one end of the rectangular simulation cell. Overall dimensions of the simulation box were $42.90\text{\AA} \times 42.90\text{\AA} \times 681.48\text{\AA}$. The space that is empty after the Fe (110) slab along the z-direction is the vacuum gap. Such large vacuum gap along the z-direction was taken to remove the interactions between periodic images in the z-direction.

The initial input model configuration for the MD simulation was made in the following way. One OH-BT (adsorbate) molecule was dispersed into eighteen

paraffin oil molecules (1:18 ratio) by using the amorphous builder in MAPS 4.1. These molecules were placed adjacent to the Fe (110) slab surface at an appropriate initial density. The atoms making up the Fe (110) were not fixed and owing to thermal noise they were vibrating (about their mean positions) throughout the simulation. The adsorbate and dispersion medium configuration was subjected to initial optimization by the conjugate gradient approximation approach. This model is henceforth denoted as system A in the rest of the manuscript.

The other three models for OH-BTS, H-NT and OH-NT molecules in paraffin oil were also constructed in the same way as system A. PCFF force field (given in MAPS 4.1) was applied on these models. The non-bonded interactions between Fe atoms and adsorbate/PO molecules were modeled by the 9–6 potential Lennard-Jones (LJ) potential in the PCFF force field [Plimpton et al. (1995)]. The PCFF force field used was modified by adding Fe-C and Fe-H LJ interaction parameters from reference [Ta et al. (2015)] for these simulations. The function below gives the van der Waal part of the PCFF force field.

$$U_{LJ} = \varepsilon \left[2 \left(\frac{\sigma}{r_{min}} \right)^9 - 3 \left(\frac{\sigma}{r_{min}} \right)^6 \right] \quad 2.2$$

In the above function ε is the well-depth, σ is van der Waals radii, r_{min} is the distance between atom type.

Each model was subjected to molecular dynamics (MD) simulation in the NVE ensemble for 20 nanoseconds using a time step of 1 femtosecond. Coulomb interactions were simulated with the particle mesh approach using a cut off distance of 12 Å. The initial temperature was $T = 298.15$ K. LAMMPS [Wilburn et al. (1978)]

program was used to run the MD simulations. The potential energy of adsorption of the adsorbate molecules on to the Fe (110) surface in the presence of dispersing medium was calculated in the following way. Results of the interacting models mentioned above were compared with non-interacting simulation or reference model. The reference model potential energy was the sum of equilibrium (long-time average) energies of the separate system of solute molecules only, the bare slab system and separate system of solvent molecules. Simulations for all component reference models were also run for 20 nanoseconds under identical NVE ensemble conditions.

2.3. Tribological Characterization

2.3.1. Steel ball

The balls of 12.7 mm diameter made up of AISI 52100 alloy steel having hardness 59-61 HRc were used for the tests. Before and after each test, balls were cleaned with n-hexane and thoroughly air-dried.

2.3.2. Base oil

The lubricating base oil, neutral liquid paraffin oil (Qualigens Fine Chemicals, Mumbai, India) having specific gravity 0.82 at 25 °C, kinematic viscosity at 40 and 100 °C as 30 and 5.5 cSt respectively, viscosity index 122, cloud point -2 °C, pour point -8 °C, flash point 180 °C and fire point 200 °C, was used without further purification.

The polyethylene glycol (PEG-200, Molecular weight 200 approx., density 1.13 gmL⁻¹, kinematic viscosity at 40 °C and 100 °C, 22.4 and 4.1 cSt respectively,

viscosity index 70, pour point -45 °C and flash point 172-185 °C) was used as a synthetic base oil.

2.3.3. Tribological Test

The tribological tastings were performed according to ASTM D4172 and ASTM D5183 standards using Four-Ball Tester, Ducom Instrument Pvt. Ltd., Bangalore, India. The antiwear tests were performed at 1200 rpm, 392 N applied load for 60 min according to ASTM D4172 standard. As per ASTM D5183 norms (successive addition of 98 N load after every 10 minutes), step loading tests were conducted until a seizure load is obtained. Besides this, to calculate wear rate, the tribological tests have also been also performed at different time intervals 15, 30, 45, 60, 75 and 90 min respectively at 392N load. All of the antiwear and load-bearing tests were performed in triplicate, and their mean values were used.

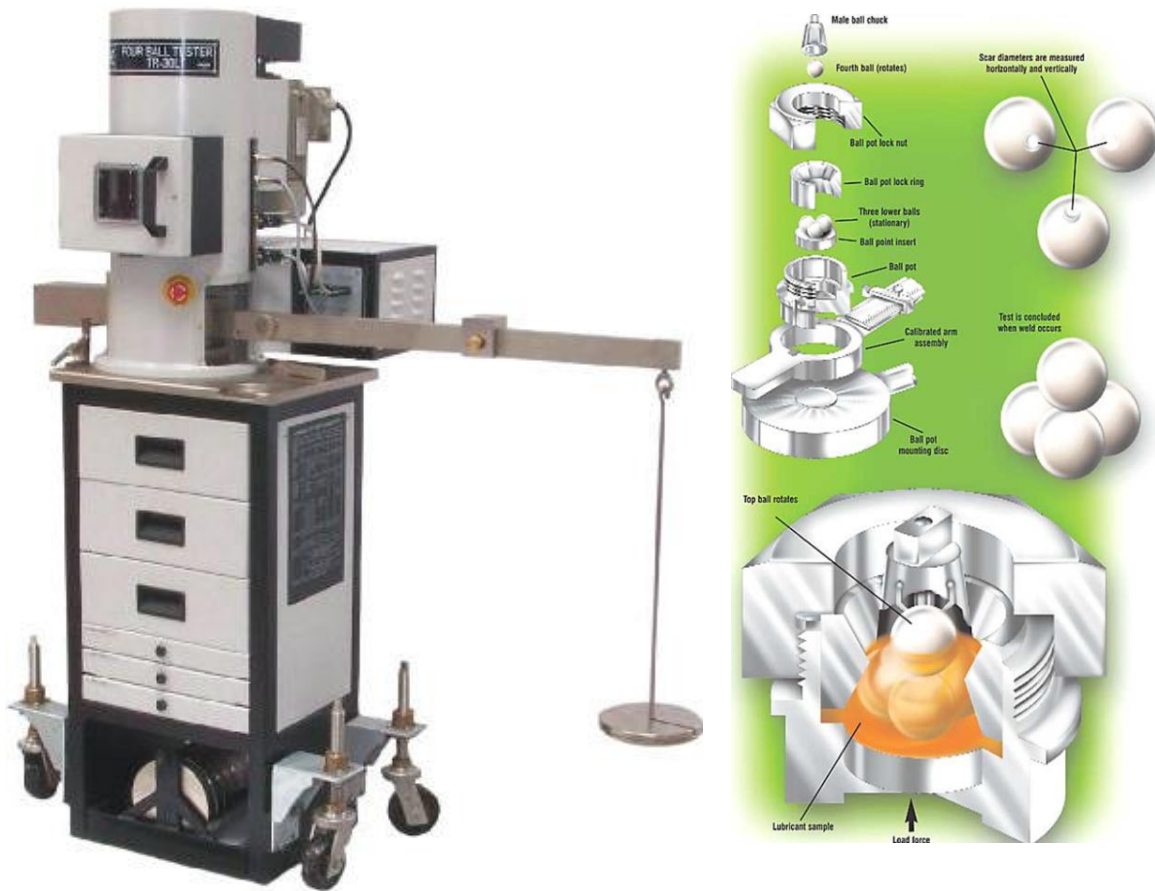


Fig. 2.1. Four-ball lubricant tester

2.3.3.1. Tribological Parameters

2.3.3.1.1. Mean wear scar diameter (MWD)

The wear scar diameter of each of the three horizontal balls was measured in two mutually perpendicular directions, one in the sliding direction (d_s) and the other perpendicular (d_p) to it using an optical microscope. The geometric mean of the two perpendicular diameters on the same ball was taken as given by the equation 2.2.

$$d_1 = \sqrt{(d_s d_p)} \tag{2.3}$$

$$d = \frac{d_1 + d_2 + d_3}{3} \tag{2.4}$$

For each experiment arithmetic mean of the above diameter of each ball (d_1 , d_2 and d_3) was taken as given by equation 2.3. The three stationary balls were not disturbed while taking the readings and the wear scar diameter was taken by tilting eyepiece of the microscope at an angle of 35.26° making it perpendicular to the surface of the scar.

2.3.3.1.2. Coefficient of friction (μ)

The coefficient of friction for different antiwear additives is obtained directly from the software of four-ball tester using equation (4)

$$F = \mu \times N$$

2.5

Where μ = Coefficient of friction, F = Frictional force, and N= Normal force

2.3.3.1.3. Mean wear volume (MWV)

$$\text{Wear volume, } V = \frac{\Pi d_0^4}{64r} \left\{ \left(\frac{d}{d_0} \right)^4 - \left(\frac{d}{d_0} \right) \right\} \quad 2.6$$

$$\text{Hertzian diameter, } d_0 = 2 \left(\frac{3Pr}{4E} \right)^{\frac{1}{3}} \quad 2.7$$

$$\text{Where, } \frac{1}{r} = \frac{1}{r_1} + \frac{1}{r_2}$$

$$\frac{1}{E^*} = \frac{1 - \nu_1^2}{E_1} + \frac{1 - \nu_2^2}{E_2}$$

Where, E^* = Resultant modulus of elasticity

ν = Poissons ratio

r = Radius of steel ball

$$E_1 = E_2 = 206 \text{ GPa}$$

$$\nu_1 = \nu_2 = 0.3$$

P = Actual load in Newton on each of the three horizontal balls that is 0.408 times of applied load.

2.3.3.1.4. Wear rate

Mean wear volume in absence and presence of different additives at 392N load for paraffin oil was plotted as a function of time, and a linear regression model was fitted to find out overall, running-in and steady-state wear rate.

2.3.3.1.5. Load- bearing capacity

Load-bearing capacity is obtained in terms of seizure load by ASTM D5183 test. The load at which frictional torque is very high and lubricant fails to sustain the load, is termed as seizure load.

2.3.3.1.6. Frictional power loss

The frictional power loss has been calculated from antiwear tests using the following relationship

$$\mathbf{P = T.\omega} \quad 2.8$$

Where P is the frictional power loss (N.m.s^{-1}), T is frictional torque and ω is the angular velocity (rad/sec).

Frictional torque T (N. m) = $F.r$; F = Frictional force and r = frictional radius = 3.662×10^{-3} (m)

Frictional force $F = \mu \cdot N$; μ = coefficient of friction and N = contact load on the three balls

$N = 1.22475L$; L is applied load (392 N)

Now $T = \mu \cdot N \cdot r$

$\omega = \pi d n / 60$; d frictional radius = $2r$ and $n = 1200$ rpm

Substituting all values in Eq. [1], the frictional power loss is

$$P = 221 \times \mu \text{ (W)} \quad 2.9$$

$$1 \text{ kWh} = 3.6 \text{ MJ} \quad 2.10$$

The antiwear test was performed under a load of 392 N at 1200 rpm for 1h using a four-ball tester. The total sliding distance of 1.656 km was covered during each test run.

2.3.3.2. Analysis of the worn surface

After each test, the balls were cleaned with n-hexane and thoroughly air-dried. One of the three lower balls was ultrasonically cleaned in n-hexane for about 5 min and allowed to dry in the atmosphere. The XPS, SEM/EDS and AFM of wear scar on this ball were recorded.

2.3.3.2.1. Scanning Electron Microscopy (SEM)

In order to understand the lubrication mechanism and morphological features of the worn surface, SEM is a very prominent technique Scanning electron microscopy

(SEM) images of the worn surface areas of the steel balls were taken using a ZEISS SUPRA 40 electron microscopy.

2.3.3.2.2. Energy Dispersive X-ray Spectroscopy (EDX)

The elemental composition of the tribofilm was studied using, ZEISS SUPRA 40 electron microscope Netherlands which gives preliminary confirmation regarding the tribochemical reaction to form *in situ* protective film.

2.3.3.2.3. Atomic Force Microscopy (AFM)

Contact mode Atomic Force Microscope (Model No. BT 02218, Nanosurf easyscan2 Basic AFM, Switzerland) was used to investigate roughness of the worn surfaces with Si₃N₄ cantilever (Nanosensor, CONTR type) having spring constant of ~0.1 Nm⁻¹ and tip radius more than 10 nm.

2.3.3.2.4. X-ray Photoelectron Spectroscopy (XPS)

The X-ray Photoelectron Spectroscopy was used for analyzing the tribofilm formed on the worn steel surface. XPS spectrometer (Thermo VG Scientific) was used to record the samples. The radiation source Al K α line with the energy of (1486.6 eV) and the binding energy of C1s (284.6 eV) was used for the calibration of the spectrometer.

SEM micrograph of steel ball and its surface roughness (AFM) are given in figure 2.2

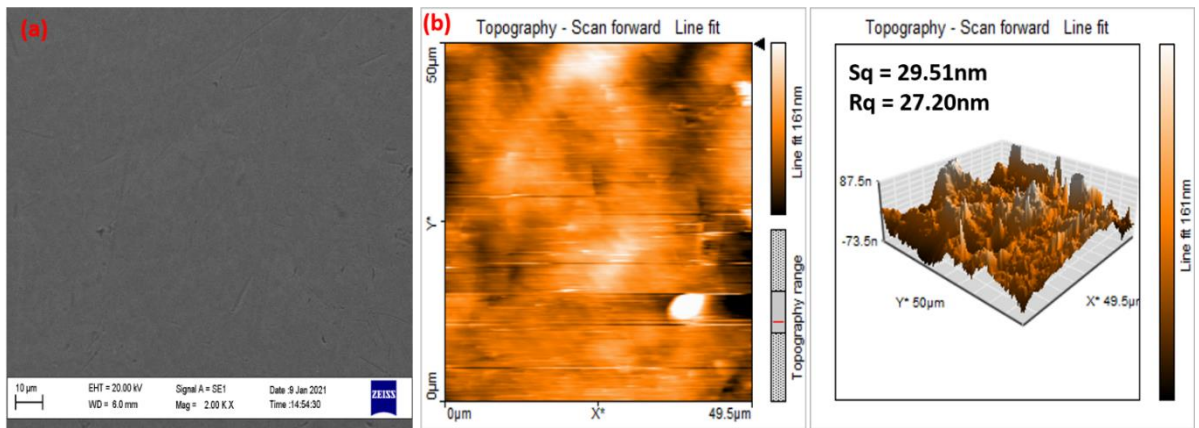


Fig. 2.2. (a) SEM micrograph (magnification 2.00k X) and (b) 2D and 3D AFM images of the plain steel ball

